Lossless microwave photonic delay line using a ring resonator with an integrated semiconductor optical amplifier

Yiwei Xie[1], Leimeng Zhuang[1], Klaus-Jochen Boller[2] and Arthur James Lowery[1,3]

[1] Electro-Photonics Laboratory, Department of Electrical and Computer Systems Engineering, Monash University, Clayton, VIC 3800, Australia
[2] Laser Physics and Nonlinear Optics group, University of Twente, PO Box 217, Enschede, 7500 AL, The Netherlands
[3] Centre for Ultrahigh-bandwidth Devices for Optical Systems (CUDOS), Monash University, Australia

E-mail: leimeng.zhuang@monash.edu

Abstract

Optical delay lines implemented in photonic integrated circuits (PICs) are essential for creating robust and low-cost optical signal processors on miniaturized chips. In particular, tunable delay lines enable a key feature of programmability for the on-chip processing functions. However, the previously investigated tunable delay lines are plagued by a severe drawback of delay-dependent loss due to the propagation loss in the constituent waveguides. In principle, a serial-connected amplifier can be used to compensate such losses or perform additional amplitude manipulation. However, this solution is generally unpractical as it introduces additional burden on chip area and power consumption, particularly for large-scale integrated PICs. Here, we report an integrated tunable delay line that overcomes the delay-dependent loss, and simultaneously allows for independent manipulation of group delay and amplitude responses. It uses a ring resonator with a tunable coupler and a semiconductor optical amplifier in the feedback path. A proof-of-concept device with a free spectral range of 11.5 GHz and a delay bandwidth in the order of 200 MHz is discussed in the context of microwave photonics and is experimentally demonstrated to be able to provide a lossless delay up to 1.1 to a 5 ns Gaussian pulse. The proposed device can be designed for different frequency scales with potential for applications across many other areas such as telecommunications, LIDAR, and spectroscopy, serving as a novel building block for creating chip-scale programmable optical signal processors.

Keywords: photonic integrated circuits, tunable delay lines, ring resonator, semiconductor optical amplifier

(Some figures may appear in colour only in the online journal)

1. Introduction

Photonic integrated circuit (PIC) technology enables the integration of complex optical systems on miniaturized chips with extremely high and long-term stability, ultimate control precision, and strong potential for low-cost fabrication. These features are crucial for the development of optical devices for many areas, such as telecommunications, LIDAR, and spectroscopy [1]. Currently, the business model of generic foundries and multi-project wafer runs rapidly advances PICs by providing industry and academia access to state-of-the-art technology platforms. In the last decade, a large number of photonic chip designs have been reported, demonstrating functions such as analog and digital processing, interconnects, sensing, energy-conversion and storage, and information interrogation [2–6].

1

Integrated optical delay lines are an essential component for creating integrated signal processing functions. In particular, tunable delay lines enable a key feature of programmability that opens a large application variety for those functions. One promising application, for example, is the integrated optical beamforming network for wideband phased array antennas required for the next generation of mobile communications [7–10], where the independent manipulation of signal amplitude and delay forms the heart of beamforming and beamsteering functions. A typical solution for such independent manipulation is interferometric filters. The reason is that these need only fulfill a generalized set of Kramers–Kronig relation whose amplitude (power transmission) and phase (group delay) responses can be independently synthesized, unlike, e.g. absorptive filters that have to obey the amplitude-phase dependency (Hilbert transform pair) of the standard Kramers–Kronig relation [11–13]. Typical implementations of interferometric filters are Bragg gratings [14], photonic crystals [15], whispering-gallery-mode resonators [16], and ring resonators [17, 18]. From an engineering perspective, ring resonators offer three advantages: (1) they can straightforwardly be fabricated using current waveguide technology; (2) the design can be extended towards serial and parallel network topologies such as CROWS (coupled resonators optical waveguide) [19, 20] and SCISSORS (side-coupled integrated spaced sequence of resonators) [21, 22], offering a large flexibility in composing desired delay line characteristics; (3) multiple tuning elements can be implemented as desired, which is of particular importance for creating programmable on-chip optical signal processors [23, 24].

To date, many integrated ring resonator delay lines have been reported using various circuit configurations and technologies. However, these delay lines are plagued by a severe drawback of delay-dependent loss due to the propagation loss in the constituent waveguides. In particular, this drawback impedes the implementation of long delays, e.g. in the order of nanoseconds (equivalent to a waveguide length of tens of centimeters), typically required by microwave photonic applications. In principle, a straightforward way to compensate such losses is to use external optical amplifiers. However, this simultaneously incurs two critical issues in practice, i.e. circuit complexity and power consumption, particularly for systems comprising many delay lines and requiring significant delays (e.g. a 16×1 optical beamforming network for K_u-band phased array antenna [7–9]).

Here, we propose and show a proof-of-concept experimental demonstration of an integrated tunable delay line that overcomes the delay-dependent loss and simultaneously allows for independent manipulation of its group delay and amplitude responses. The delay line uses a ring resonator in an all-pass filter architecture with a tunable coupler and a semiconductor optical amplifier (SOA) [26] in the feedback path. As a key feature, when providing a lossless delay, the SOA in this work needs only to provide a gain that compensates the device waveguide loss, i.e. waveguide propagation loss of one resonator roundtrip regardless of delay value, whereas using an external optical amplifier will require a gain nearly equal to the multiplication of the device waveguide loss and the delay value in terms of the number of
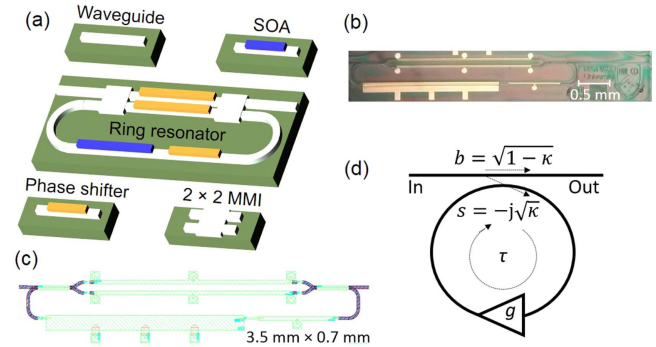

Figure 1. Device description. (a) A schematic, (b) the mask layout design, and (c) a photomicrograph of the novel device. (d) An illustration of the signal processing operation.

resonator roundtrips. While ring resonators incorporating SOAs have been investigated for optical signal processing, e.g. ring resonators in add-drop multiplexer architecture as spectral filters [25], and coupled ring resonators as integrators, Hilbert transformers, and differentiators [27, 28] featuring arbitrary evaluation of the device transfer function [29], a ring resonator delay line in an all-pass filter architecture that utilizes a SOA to control the feedback-path amplitude factor opens a novel building block for chip-scale processors of tunability, i.e. allowing for loss, all-pass (lossless), or gain in the delay passband. This new tunability breaks the paradigm of previously demonstrated ring resonator delay lines that are restricted to delay passband losses. The proof-of-concept device of this work shows a delay bandwidth in the order of 200 MHz, which is discussed in the context of microwave photonics. However, such devices can be designed for different frequency scales with potential for applications across many other areas such as telecommunications, LIDAR, and spectroscopy, serving as a novel building block for creating chip-scale programmable optical signal processors.

2. Device description

Figure 1(a) shows the construction of the novel delay line. It comprises a ring resonator that incorporates a SOA in the feedback path. Coupling to the bus waveguide is implemented as a Mach–Zehnder interferometer (MZI) structure comprising two 2-by-2 3 dB multimode interferometer couplers. The power coupling is controlled by means of phase shifters in the arms of the MZI [4, 17, 18]. An additional phase shifter is placed in the feedback path to enable control of its resonant frequency. The chip is fabricated in an indium phosphide waveguide platform [30]. The SOA in the cavity is constructed using an InGaAsP/InP quantum well with a size of $2000 \times 2\ \mu\mathrm{m}^2$ and has a polarization-independent gain controlled by a bias current. The threshold current density for onset of gain is $0.5\ \mathrm{kA\ cm}^{-2}$ and the saturation current density is $7\ \mathrm{kA\ cm}^{-2}$ where the gain coefficient amounts to about $70\ \mathrm{cm}^{-1}$. The passive waveguide in the device has a propagation loss of about $3.5\ \mathrm{dB\ cm}^{-1}$ and the coupling loss to the single-mode lensed fiber (OZ Optics) used in the experiment

is about 5 dB per facet. The resonator has a free spectral range, f_{FSR}, of 11.5 GHz. Figures 1(b) and (c) show the mask layout design and a photomicrograph of the fabricated device.

Using the digital-filter-modeling method as explained in [29], the signal processing operation of the device can be described by a schematic as shown in figure 1(d), whose time-domain discrete impulse response is given by

$$h(t) = b\delta(t) - s^2 g\delta(t - \tau) - \cdots - s^2 g^n \delta(t - n\tau), \quad (1)$$

where $\delta(t)$ is the delta function, $n = \infty$, $b = \text{sqrt}(1-\kappa)$ and $s = -j\text{sqrt}(\kappa)$ are respectively the coupler's bar- and cross-port amplitude factors with $\kappa \in [0, 1]$ being the power coupling coefficient, $g \in (0, +\infty)$ the feedback-path amplitude factor of the resonator which represents the net effect of the waveguide propagation loss and SOA gain in the feedback path, and $\tau = 1/f_{FSR}$ is the roundtrip delay of the cavity. The frequency-domain characteristic of the device can be described using its z-transform:

$$H(z) = b - (1 - b^2)(gz^{-1} + g^2 z^{-2} + \cdots + g^n z^{-n})$$
$$= \frac{b - gz^{-1}}{1 - bgz^{-1}} = \frac{b(z - g/b)}{(z - bg)} \quad (2)$$

which has $z = \exp(j2\pi f\tau + \theta)$ with f the frequency, θ the feedback path phase shift, $\rho = bg$ and $\sigma = g/b$ respectively expressing the magnitudes of the pole and the zero of the transfer function. The amplitude and group delay response of the device can be respectively obtained by evaluating $|H(z)|$ and the first-order derivative of $-\arc(H(z))$ with respect to f within one free spectral range.

3. Experimental results

3.1. Delay line properties

The resonator's frequency responses were measured using an optical vector analyzer (Luna System OVA5000). Figure 2 shows the measurement results, where the resonator's tuning elements, i.e. g and κ, are evaluated by means of curve-fitting of the measured responses to the theoretical calculations. For this experiment, the light intensities were kept low to avoid the SOA gain compression; besides, the variation of the resonator's overall group index due to nonlinear properties of the SOA [26] does not play a significant role as the bandwidth of interest in this work is within one free spectral range. For the result in figure 2(a), $g < 1$ is introduced by setting the SOA to have a lower gain than the waveguide loss of the feedback path, and the condition of undercoupling, i.e. $b > g$, is given so that both the pole and zero of equation (2) are located within the unit circle of the zero-pole plot, i.e. $\rho < 1$ and $\sigma < 1$. In this case, the device provides a negative group delay at the resonant frequency [29]. As explained in [13], this zero-pole relation means that the device works as a minimum-phase filter, in which a negative group delay is accompanied by a low power transmission. Although significant negative group delays can be generated for the purpose of temporal advancing of pulsed signals [31], the associated loss becomes significant as well, which hinders a practical use of this approach.
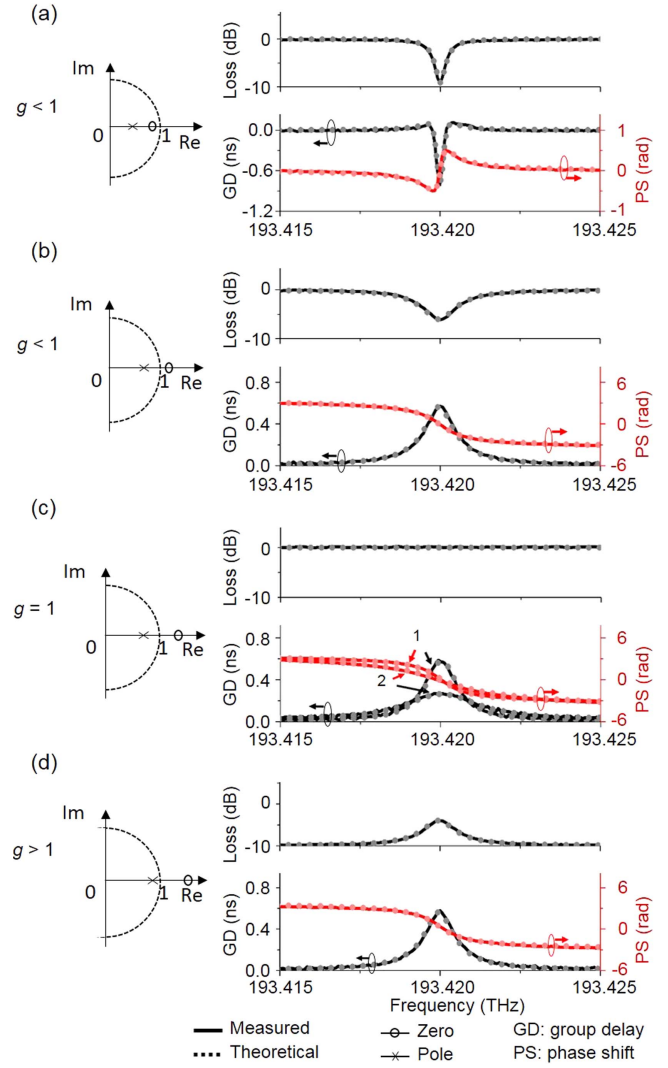

Figure 2. Measured and calculated frequency responses of the novel device for different settings of its feedback-path amplitude factor, g, and the coupling coefficient, κ. The resonant frequency is aligned to 193.42 THz with (a) $g = 0.87$ and $\kappa = 0.1$ ($b = 0.95$), (b) $g = 0.87$ and $\kappa = 0.49$ ($b = 0.71$), (c) $g = 1$ and $\kappa = 0.49$ ($b = 0.71$) for Case 1; $\kappa = 0.8$ ($b = 0.45$) for Case 2, (d) g = 1.12 and $\kappa = 0.49$ ($b = 0.71$). Insets: zero-pole plots of equation (2).

For the case of overcoupling, i.e. $b < g$, the pole of $H(z)$ in equation (2) stays inside the unit circle, still indicating a stable system, but the zero is outside the unit circle, i.e. $\rho < 1$ and $\sigma > 1$. In this case, the device works as a non-minimum-phase filter [12], allowing independent synthesis of its amplitude and group delay responses. Utilizing this filter property and varying g using the SOA, one can generate a delay line but still independently select loss, all-pass (loss-less), or gain in the passband. Figure 2(b) shows the conventional lossy case, i.e. $g < 1$, where the device provides a positive group delay and a passband loss, both having a Lorentz-model shape as can be seen from the functional form of equation (2) [29]. Figure 2(c) demonstrates a lossless operation enabled by the proposed device, where the SOA is set to exactly the gain that compensates the waveguide loss of the feedback path, i.e. $g = 1$. In this case, the device works as
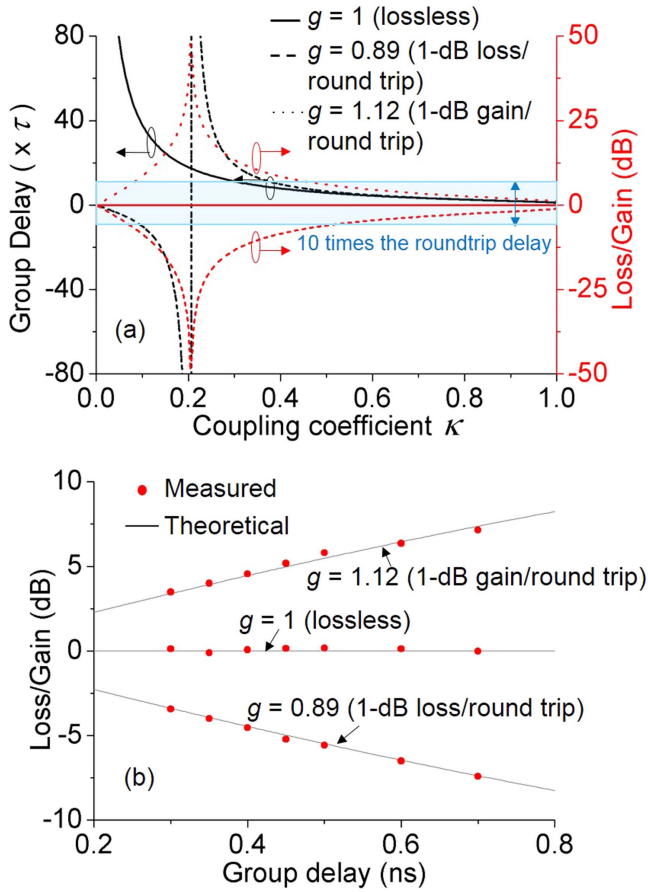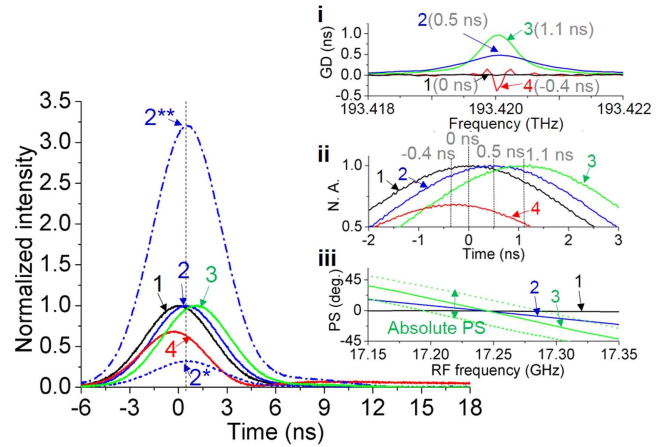
Figure 4. Demonstration of timing and amplitude variation of pulsed signals implemented using the proposed device as a tunable delay line. Insets: (i) the device's group delay responses implemented in the experiment, (ii) zoom-in view of the output pulses, and (iii) a demonstration of RF delay line function.

Figure 3. Device characteristics. (a) Calculations of group delay and loss (or gain) at the resonant frequency versus the feedback-path amplitude factor, g (the ratio between SOA gain in the feedback path and the waveguide propagation loss), and the coupling coefficient, κ. (τ is the roundtrip delay) (b) experimental verification of loss/gain-group delay relation of the device.

an optical all-pass filter whose transfer function features a numerator and a denominator being a reverse-polynomial pair with respect to the argument z. Such a filter provides a unity amplitude response but a positive group delay controlled by the coupling κ (or by b in terms of equation (2)) [29]. Finally, figure 2(d) shows the case with the same coupling as in figure 2(b), but with g being reciprocal to that case with $g > 1$ and $\sigma < 1$. In effect, the passband loss is inverted into a passband gain without changing the group delay, such that the filter fulfills $|H(g)| = 1/|H(1/g)|$. A mathematical explanation of this property is that the numerator and denominator of equation (2) are a conjugate-reciprocal-polynomial pair with respect to the argument g. A situation which is outside the scope of this work and therefore will not be discussed here is when g is increased further such that $g > \kappa$. In this case the SOA gain is so large that it exceeds the overall roundtrip loss of the resonator including both waveguide loss and the coupling, i.e. the resonator will be driven into the laser oscillation. The results summarized in figure 2 verify the tunable delay line function of the proposed device in which the variability of both g and κ enables the independent synthesis of its amplitude and group delay response.

Using equation (2), the group delay and loss (or gain) at the resonant frequency of the resonator can be calculated as a function of κ and g. Figure 3(a) displays these calculations that were carried across the tuning range of κ for three representative cases of g. It shows that the group delay and the accompanying loss (or gain) have a nearly linear relation to κ when the group delay is shorter than 10 times the roundtrip delay of the resonator, but a nearly exponential relation to κ when larger than that. In practice, such a delay line should be operated in the nearly linear regime to improve control accuracy as the latter regime imposes more stringent requirements for the precision of κ, which should be taken into account for the design of resonator roundtrip delay that determines the device size. As a verification of the delay line operating in the nearly linear regime, seven group delays were measured for the three cases of g using the proposed device; the results presented in figure 3(b) show excellent agreement to the calculations.

3.2. Delay effect measurements

Figure 4 shows the time-domain pulse measurements demonstrating the delay line function of the proposed device. As the input signal, a transform-limited (chirp-free) Gaussian-envelop optical pulse train characterized by a pulse FWHM of 5 ns and an interval of 100 ns was sent into the device, with the light center frequency aligned to the resonant frequency at 193.42 THz. The optical pulses were generated by modulating a CW light (Alnair Labs) using a Mach–Zehnder intensity modulator (Sumitomo Industry 40 Gb s^{-1}) driven by an 5 ns electrical pulse train from an arbitrary waveform generator (Tektronix AWG7102); the device output was detected using a DC-coupled photodetector (Discovery DSC-40 s); and the time-domain waveform was measured using a 28 GHz digital storage oscilloscope (Agilent DSO 92804A). For clarity, figure 4(i) presents the device's group delay responses implemented in the experiment, and figure 4(ii) shows the zoom-in view of the corresponding output pulses in the time

domain. To obtain these results, first, $g = 1$ was applied to the device in association with the implementation of three different group delay peaks (by varying κ), i.e. Cases 1, 2, and 3 as shown in figure 4(i). In the time domain as shown in figure 4(ii), the output pulse of Case 1 is used as the reference corresponding to $\kappa = 0$ (meaning that the ring resonator is actually decoupled from the bus waveguide and the device reduces to an equivalent of a straight waveguide), and the output pulses of Case 2 and 3 have the same peak intensities and corresponding timing delays. These results verify the successful implementation of a tunable delay line free of delay-dependent losses. Then, we configured the device with the group delay response of Case 2 and tuned the SOA gain to provide the statuses of $g < 1$ (loss) and $g > 1$ (gain). As shown by '2*' and '2**' in figure 4, this practice leads to attenuation or amplification of the output pulse, respectively, without changing the pulse timing. This result demonstrates the independent manipulation of signal amplitude. In addition, the effect of the device's negative group delay, i.e. Case 4 in figure 4(i), was also demonstrated where the corresponding output pulse reduced to an attenuated version with a relative timing advance [31] as shown in figure 4(ii).

As another application example, the device was used in a microwave photonic link with a RF bandwidth of 200 MHz centered at 17.25 GHz. A probe RF signal was modulated onto a lightwave using the same laser and modulator. A single-sideband modulation spectrum was applied into the device, which was generated by means of a spectral filter (Finisar WaveShaper 4000) with one sideband aligned to a resonant frequency of the device. The RF probe signal generation and the system RF response measurements were performed using an electrical vector network analyzer (Anritsu 37247D). When tuning the device between Cases 1–3 as shown in figure 4(i), the frequency response of the detected RF signal changes accordingly as shown in figure 4(iii), i.e. tuning the delay changes the linear slope of the RF phase shift. In addition, the device is also able to introduce an absolute RF phase shift by changing the resonant frequency relative to the RF sideband, the implementation of which can be done by using the phase shifter in the resonator feedback path, or by changing the frequency of the optical carrier.

4. Conclusion

In conclusion, we have experimentally demonstrated a lossless delay line using an integrated ring resonator with a SOA in its feedback path. For the proof-of-concept purpose, our experiment employed a single ring resonator fabricated via a generic foundry service, which shows a limited bandwidth (due to a constant delay-bandwidth product governed by the Lorentz-model shape of the group delay response) and a device size of $3.5 \times 0.7 \text{ mm}^2$. However, previous studies on integrated delay lines have shown possible solutions to improve these aspects, e.g. a bandwidth broadening can be implemented by using multiple ring resonators in CROW or SCISSOR configurations [19–22], and a more compact design of SOA can be used to reduce the device size [24]. For

optimum device performance, the operating light intensity should consider of the SOA gain compression and the noise from the SOA spontaneous emission [26]. Regarding device functions, a single ring resonator is not able to provide negative group delays in combination with gain because with the required parameter settings the laser threshold would be surpassed. However, it has been predicted theoretically that a PIC topology of a network of coupled ring resonators with gain control [32] can provide an analogous response as dielectric media that support gain-assisted superluminal propagation of light [33]. A successful on-chip demonstration of this prediction would stimulate the exploration of novel directions in physics, and equally important, inspire new engineering applications of such devices. The tunable delay line function of the proposed device, demonstrated here with experimental results, show the basic ingredients to obtain the capability of independent manipulation of amplitude and group delay responses, and serves as a novel building block for various types of PIC topologies such as chip-scale programmable optical signal processors [23].

References

[1] Andrews D L 2015 *Photonics Volume 3: Photonics Technology and Instrumentation* (New York: Wiley)

[2] Doerr C R 2015 Silicon photonic integration in telecommunications *Front. Phys.* **3** 37

[3] Heck M J R, Bauters J F, Davenport M L, Doylend J K, Jain S, Kurczveil G, Srinivasan S, Tang Y and Bowers J E 2013 Hybrid silicon photonic integrated circuit technology *J. Sel. Top. Quantum Electron.* **19** 6100117

[4] Roeloffzen C G H, Zhuang L, Taddei C, Leinse A, Heideman R G, van Dijk P W L, Oldenbeuving R M, Marpaung D A I, Burla M and Boller K-J 2013 Silicon Nitride microwave photonic circuits *Opt. Express* **21** 22937–61

[5] Wörhoff K, Heideman R G, Leinse A and Hoekman M 2015 TriPleX: a versatile dielectric photonic platform *Adv. Opt. Technol.* **4** 189–207

[6] Smit M, van der Tol J and Hill M 2012 Moore's law in photonics *Laser Photon. Rev.* **6** 1–13

[7] Meijerink A *et al* 2010 Novel ring resonator-based integrated photonic beamformer for broadband phased array receive antennas: I. Design and performance analysis *J. Lightwave Technol.* **28** 3–18

[8] Zhuang L, Roeloffzen C G, Meijerink A, Burla M, Marpaung D A I, Leinse A, Hoekman M, Heideman R G and van Etten W 2010 Novel ring resonator-based integrated photonic beamformer for broadband phased array antennas: II. Experimental prototype *J. Lightwave Technol.* **28** 19–31

[9] Burla M, Marpaung D A I, Zhuang L, Khan M R, Leinse A, Beeker W P, Hoekman M, Heideman R G and Roeloffzen C G H 2013 Multiwavelength-integrated optical beamformer based on wavelength division multiplexing for 2D phased array antennas *J. Lightwave Technol.* **32** 3509–20

[10] Zhuang L *et al* 2014 On-chip microwave photonic beamformer circuit operating with phase modulation and direct detection *Opt. Express* **22** 17079–91

[11] Kop R H J, de Vries P, Sprik R and Lagendijk A 1997 Kramers–Kronig relations for an interferometer *Opt. Commun.* **138** 118–26

[12] Wang L J 2002 Causal 'all-pass' filters and Kramers–Kronig relations *Opt. Commun.* **213** 27–32

[13] Lenz G, Eggleton B J, Giles C R, Madsen C K and Slusher R E 1998 Dispersive properties of optical filters for WDM systems *IEEE J. Quantum Electron.* **34** 1390–420

[14] Wang J, Ashrafi R, Adams R, Glesk I, Gasulla I, Capmany J and Chen L R 2016 Subwavelength grating enabled on-chip ultra-compact optical true time delay line *Sci. Rep.* **6** 30235

[15] Sancho J *et al* 2012 Integrable microwave filter based on a photonic crystal delay line *Nat. Commun.* **3** 1075

[16] Asano M, Özdemir S K, Chen W, Ikuta R, Yang L, Imoto N and Yamamoto T 2016 Controlling slow and fast light and dynamic pulse-splitting with tunable optical gain in a whispering-gallary-mode microcavity *Appl. Phys. Lett.* **108** 181105

[17] Zhuang L, Hoekman M, Beeker W P, Leinse A, Heideman R G, van Dijk P W L and Roeloffzen C G H 2013 Novel low-loss waveguide delay lines using Vernier ring resonator for on-chip multi-λ microwave photonic signal processors *Laser Photon. Rev.* **7** 994–1002

[18] Burla M, Marpaung D A I, Zhuang L, Roeloffzen C G H, Khan M R, Leinse A, Hoekman M and Heideman R G 2011 On-chip CMOS compatible reconfigurable optical delay line with separate carrier tuning for microwave photonic signal processing *Opt. Express* **19** 21475–84

[19] Bogaerts W, de Heyn P, van Vaerenbergh T, de Vos K, Selvaraja S K, Claes T, Dumon P, Bienstman P, van Thourhout D and Baets R 2012 Silicon microring resonator *Laser Photon. Rev.* **6** 47–73

[20] Morichetti F, Ferrari C, Canciamilla A and Melloni A 2012 The first decade of coupled resonator optical waveguides: bringing slow light to applications *Laser Photon. Rev.* **6** 74–96

[21] Cardenas J, Foster M A, Sherwood-Droz N, Poitras C B, Lira H L R, Zhang B, Gaeta A L, Khurgin J B, Morton P and Lipson M 2010 Wide-bandwidth continuously tunable optical delay line using silicon microring resonators *Opt. Express* **18** 26525–34

[22] Capmany J, Domenech D and Muñoz P 2015 Silicon graphene reconfigurable CROWS and SCISSORS *IEEE Photon. J.* **7** 2700609

[23] Zhuang L, Roeloffzen C G H, Hoekman M, Boller K-J and Lowery A J 2015 Programmable photonic signal processor chip for radiofrequency applications *Optica* **2** 854–9

[24] Liu W, Li M, Guzzon R S, Norberg E J, Parker J S, Lu M, Coldren L A and Yao J 2016 A fully reconfigurable photonic integrated signal processor *Nat. Photon.* **10** 190–5

[25] Rabus D G, Hamacher M, Troppenz U and Heidrich H 2002 Optical filters based on ring resonators with integrated semiconductor optical amplifiers in GaInAsP–InP *IEEE J. Sel. Top. Quantum Electron.* **8** 1405

[26] Rostami A, Baghban H and Maram R 2010 *Nanostructure Semiconductor Optical Amplifier: Building Blocks for All-Optical Processing* (Berlin: Springer)

[27] Guzzon R S, Norberg E J, Parker J S, Johansson L A and Coldren L A 2011 Integrated InP–InGaAsP tunable coupled ring optical bandpass filters with zero insertion loss *Opt. Express* **19** 7816–26

[28] Liu W, Li M, Guzzon R S, Norberg E J, Parker J S, Coldren L A and Yao J 2014 A photonic temporal integrator with an ultra-long integration time window based on an InP–InGaAsP integrated ring resonator *J. Lightwave Technol.* **32** 3654–9

[29] Madsen C K and Zhao J H 1999 *Optical Filter Design and Analysis: A Signal Processing Approach* (New York: Wiley)

[30] www.smartphotonics.nl

[31] Uranus H P, Zhuang L, Roeloffzen C G H and Hoekstra H J W M 2007 Pulse advancement and delay in an integrated optical two-port ring-resonator circuit: direct experimental observations *Opt. Lett.* **32** 2620–2

[32] Wang L J, Kuzmich A and Dogariu A 2000 Gain-assisted superluminal light propagation *Nature* **406** 277–9

[33] Chang H and Smith D D 2005 Gain-assisted superluminal propagation in coupled optical resonators *J. Opt. Soc. Am.* B **22** 2237–41